AIP | APL Materials
NOW INDEXED IN THOMSON REUTERS DATABASES

Slanted n-ZnO/p-GaN nanorod arrays light-emitting diodes grown by oblique-angle deposition

Ya-Ju Lee, Zu-Po Yang, Fang-Yuh Lo, Jhih-Jhong Siao, Zhong-Han Xie, Yi-Lun Chuang, Tai-Yuan Lin, and Jinn-Kong Sheu

Citation: APL Materials **2**, 056101 (2014); doi: 10.1063/1.4874455
View online: http://dx.doi.org/10.1063/1.4874455
View Table of Contents: http://scitation.aip.org/content/aip/journal/aplmater/2/5?ver=pdfcov
Published by the AIP Publishing

Articles you may be interested in

Tuning the emission of ZnO nanorods based light emitting diodes using Ag doping
J. Appl. Phys. **116**, 193104 (2014); 10.1063/1.4902526

Ultraviolet electroluminescence from ordered ZnO nanorod array/p-GaN light emitting diodes
Appl. Phys. Lett. **100**, 171109 (2012); 10.1063/1.4706259

ZnO nanorod/GaN light-emitting diodes: The origin of yellow and violet emission bands under reverse and forward bias
J. Appl. Phys. **110**, 094513 (2011); 10.1063/1.3653835

Influence of the alignment of ZnO nanorod arrays on light extraction enhancement of GaN-based light-emitting diodes
J. Appl. Phys. **109**, 083110 (2011); 10.1063/1.3574441

Emission mechanisms of passivated single n-ZnO:In/i-ZnO/p-GaN-heterostructured nanorod light-emitting diodes
Appl. Phys. Lett. **97**, 111111 (2010); 10.1063/1.3490652

This article is copyrighted as indicated in the article. Reuse of AIP content is subject to the terms at: http://aplmaterials.aip.org/about/rights_and_permissions Downloaded to IP: 140.113.38.11 On: Thu, 25 Dec 2014 02:59:18

APL MATERIALS **2**, 056101 (2014)

Slanted n-ZnO/p-GaN nanorod arrays light-emitting diodes grown by oblique-angle deposition

Ya-Ju Lee,[1,a] Zu-Po Yang,[2] Fang-Yuh Lo,[3] Jhih-Jhong Siao,[1] Zhong-Han Xie,[1] Yi-Lun Chuang,[1] Tai-Yuan Lin,[4,b] and Jinn-Kong Sheu[5,c]
[1]*Institute of Electro-Optical Science and Technology, National Taiwan Normal University, 88, Sec. 4, Ting-Chou Road, Taipei 116, Taiwan*
[2]*Institute of Photonic Systems, National Chiao-Tung University, 301, Gaofa 3rd Road, Tainan 711, Taiwan*
[3]*Department of Physics, National Taiwan Normal University, 88, Sec. 4, Ting-Chou Road, Taipei 116, Taiwan*
[4]*Institute of Optoelectronic Sciences, National Taiwan Ocean University, 2, Pei-Ning Road, Keelung 202, Taiwan*
[5]*Department of Photonics, National Cheng Kung University, 1, University Road, Tainan 701, Taiwan*

(Received 10 March 2014; accepted 22 April 2014; published online 2 May 2014)

High-efficient ZnO-based nanorod array light-emitting diodes (LEDs) were grown by an oblique-angle deposition scheme. Due to the shadowing effect, the inclined ZnO vapor-flow was selectively deposited on the tip surfaces of pre-fabricated p-GaN nanorod arrays, resulting in the formation of nanosized heterojunctions. The LED architecture composed of the slanted n-ZnO film on p-GaN nanorod arrays exhibits a well-behaving current rectification of junction diode with low turn-on voltage of 4.7 V, and stably emits bluish-white luminescence with dominant peak of 390 nm under the operation of forward injection currents. In general, as the device fabrication does not involve passivation of using a polymer or sophisticated material growth techniques, the revealed scheme might be readily applied on other kinds of nanoscale optoelectronic devices. © *2014 Author(s). All article content, except where otherwise noted, is licensed under a Creative Commons Attribution 3.0 Unported License.* [http://dx.doi.org/10.1063/1.4874455]

Zinc oxide (ZnO) is a promising material for the next generation of short-wavelength (blue/near-UV) light-emitting diodes (LEDs),[1] due to its unique characteristics such as direct and wide bandgap energy of 3.37 eV, large exciton binding energy of 60 meV, and high radiation resistance for harsh environments operation.[2,3] Owing to intrinsically n-type polarity,[4,5] and difficulty in achieving reproducible and stable p-type ZnO material,[6,7] most of ZnO-based LEDs are constructed as heterojunction structures with other p-type materials.[8–12] Among them, the n-ZnO/p-GaN heterojunction is the most suggested configuration for practical applications in consideration of their same wurtzite structure with small lattice mismatch (∼1.9%) and mature development of p-type GaN in the LED industry.[13] Nevertheless, a large energy-band offset was induced at the n-ZnO/p-GaN interface,[14] hindering the electrical carrier injection, and in consequence, degrading the actual performance of the LEDs. Nanostructures such as nanowire and nanorod arrays have been widely proposed to overcome the above issue by increasing the carrier injection efficiency through nanosized junctions.[15–19] The LED's light extraction efficiency is also enhanced by virtue of the optical coupling or strong scattering of guided light with the nanostructures. But in all of these cases, making electrical contacts to nanostructured LEDs with submicrometer dimensions generally requires multiple procedures,

[a]Electronic mail: yajulee@ntnu.edu.tw
[b]Electronic mail: tylin@mail.ntou.edu.tw
[c]Electronic mail: jksheu@mail.ncku.edu.tw

 ©Author(s) 2014

This article is copyrighted as indicated in the article. Reuse of AIP content is subject to the terms at: http://aplmaterials.aip.org/about/rights_and_permissions Downloaded to IP: 140.113.38.11 On: Thu, 25 Dec 2014 02:59:18

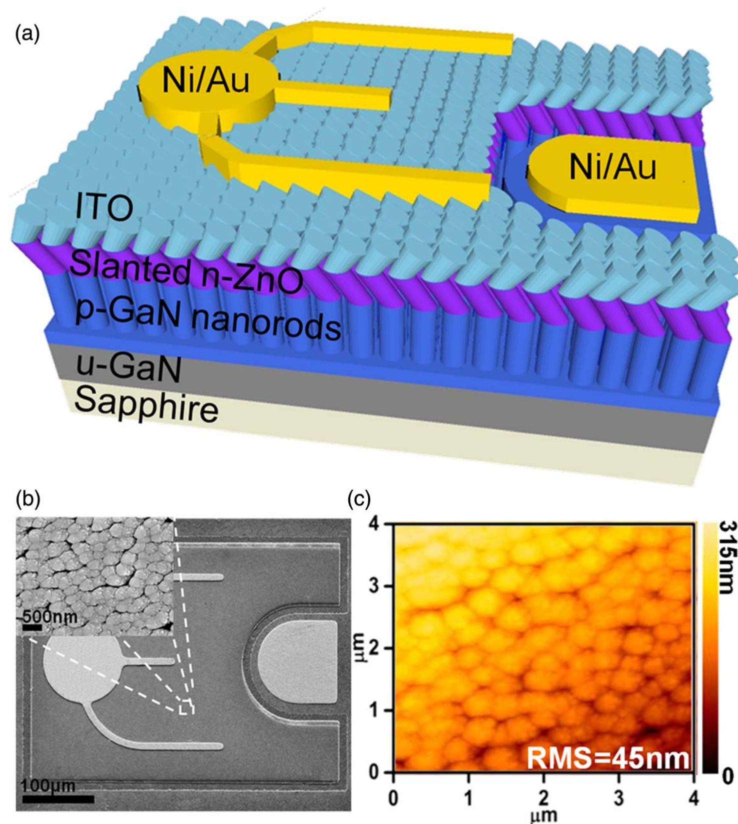

FIG. 1. (a) Design architecture of the LED composed of slanted n-ZnO film ($\theta = 60^{\circ}$, vapor-flow incident angle) on p-GaN nanorod arrays. An additional slanted ITO film ($\theta = -60^{\circ}$, vapor-flow incident angle) was grown to interconnect the slanted n-ZnO/p-GaN nanorod arrays for electrical injection. (b) A top-view SEM image of the fabricated LED. (Inset) an enlarged top-view SEM image of the surface of slanted ITO film. (c) AFM image of the slanted ITO film grown by oblique-angle deposition.

involving not only a completed filling of polymers into the interval gaps of nanorods, but a precise etching to expose the tip regions of nanorod arrays, which largely constricts their applications in high performance optoelectronic devices. Here we demonstrate a general strategy using oblique-angle deposition to fabricate the blue/near-UV LEDs composed of the slanted n-ZnO film on randomly distributed p-GaN nanorod arrays. Due to the shadowing effect provided by the pre-fabricated p-GaN nanorod arrays,[20,21] the inclined ZnO vapor-flow was selectively deposited on the tip surfaces of the nanorods, and eventually coalesced altogether to form a continuous film with good crystalline quality. As a result of proposed scheme, the fabricated slanted n-ZnO/p-GaN nanorod arrays LED exhibits a well-behaving current rectification of junction diode and strong bluish-white electroluminescence (EL). Moreover, this method allows us to overcome the constrictions of using a polymer, rendering our technique low cost and reliable for mass-production of nanoscale optoelectronic devices.

The design architecture of the proposed LED is depicted in Fig. 1(a). The 2-μm-thick undoped GaN buffer layer and 400-nm-thick p-type GaN layer were subsequently grown on a (0001) sapphire substrate by metal-organic chemical vapor deposition. The hole concentration and mobility of p-type GaN layer acquired by a four-point Hall measurement are $p = 5.5 \times 10^{17}$ cm^{-3} and $\mu_p = 6.2$ cm^2/Vs, respectively. The randomly distributed nanorod arrays were fabricated on the p-type GaN layer by using self-assembled nickel (Ni) cluster as a hard mask for inductively coupled plasma (ICP) dry etching. During ICP process, we employed the standard photolithography to further protect the p-contact region for the subsequent fabrication of p-electrode. The fabrication detail of nanorod arrays is described in Ref. 21. Figure 2(a) presents a cross-sectional scanning electron micrograph (SEM) image of fabricated p-GaN nanorod arrays. Accordingly, the p-GaN nanorod arrays with

This article is copyrighted as indicated in the article. Reuse of AIP content is subject to the terms at: http://aplmaterials.aip.org/about/rights_and_permissions Downloaded to IP: 140.113.38.11 On: Thu, 25 Dec 2014 02:59:18

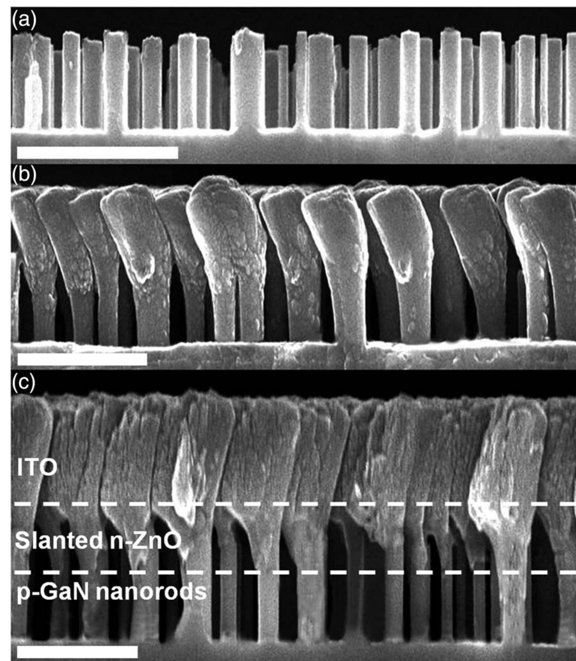

FIG. 2. Cross-sectional SEM images of (a) p-GaN nanorod arrays, (b) slanted n-ZnO/p-GaN nanorod arrays, and (c) after they were grown an additional slanted ITO film for electrical injection. The scale bars are all 500 nm.

300 nm in length are vertically aligned along the ⟨0001⟩ direction. The diameter of individual p-type GaN nanorod ranges from 100 to 140 nm, primarily determined by the deposition thickness of the Ni cluster and the ICP condition. The number density of nanorod arrays is estimated to be 2.2×10^9 cm^{-2}, which corresponds to a volume filling faction of ∼17.3%. The slanted ZnO film with 300 nm in thickness was then grown by oblique-angle deposition using a radio frequency (RF) magnetron sputtering system at room temperature, and a representative cross-sectional SEM image is shown in Fig. 2(b). In the deposition, the sample stage on which our nanorod arrays is loaded was tilted an angle of $\theta = 60^\circ$ (same as nanorod array) with respect to the ZnO vapor-flow direction. The ZnO sputtering target was 76.4 mm in diameter and 99.99% pure, and the target-substrate distance was 70 mm. The sputtering chamber was evacuated to a pressure of 5×10^{-6} torr, and then oxygen (99.99%) and argon (99.999%) were introduced as sputtering gases with a ratio of O_2 (2 sccm)/Ar (10 sccm) = 20%. The working pressure and sputtering power were kept as 8×10^{-3} torr and 100 W, respectively. As compared to other growth schemes, the oblique-angle sputtering system would provide useful advances in the production of cost-effective and nanostructured ZnO-based optoelectronic devices. Due to the shadowing effect provided by the pre-fabricated p-GaN nanorod arrays with high aspect ratio (3:1), the inclined ZnO vapor-flow is deposited selectively on the tip surfaces of the p-GaN nanorods. The grown sample was then subjected to rapid thermal annealing (RTA) at 900 °C under a nitrogen atmosphere for 1 min to alleviate the influence of intrinsic defects and interface states of slanted ZnO film on the LED's performance.[22] The doping concentration and carrier mobility of slanted ZnO film characterized by means of four-point probe and Hall measurement amount to $n = 7.4 \times 10^{18}$ cm^{-3} and $\mu_n = 3.9$ cm^2/Vs, respectively, with an n-type polarity. Finally, an additional slanted indium-tin-oxide (ITO) film with a thickness of 400 nm was again grown by the RF magnetron sputtering with an incident angle of $\theta = -60^\circ$ to interconnect the slanted n-ZnO/p-GaN nanorod arrays, and that also provides as a continuous and conductive platform for the subsequent mask-evaporation of Ni/Au n-electrode and electrical injection [Fig. 2(c)]. The measured resistivity of slanted ITO film is $\rho = 1.27 \times 10^{-3}$ Ω-cm, which is acceptable to perform as an electrical conductive film for LED applications. Thus electrons from n-electrode are spread out uniformly within the ITO layer, and then injected evenly into each individual slanted n-ZnO/p-GaN nanorods. Fig. 1(b) shows the top-view SEM image of the fabricated

This article is copyrighted as indicated in the article. Reuse of AIP content is subject to the terms at: http://aplmaterials.aip.org/about/rights_and_permissions Downloaded to IP: 140.113.38.11 On: Thu, 25 Dec 2014 02:59:18

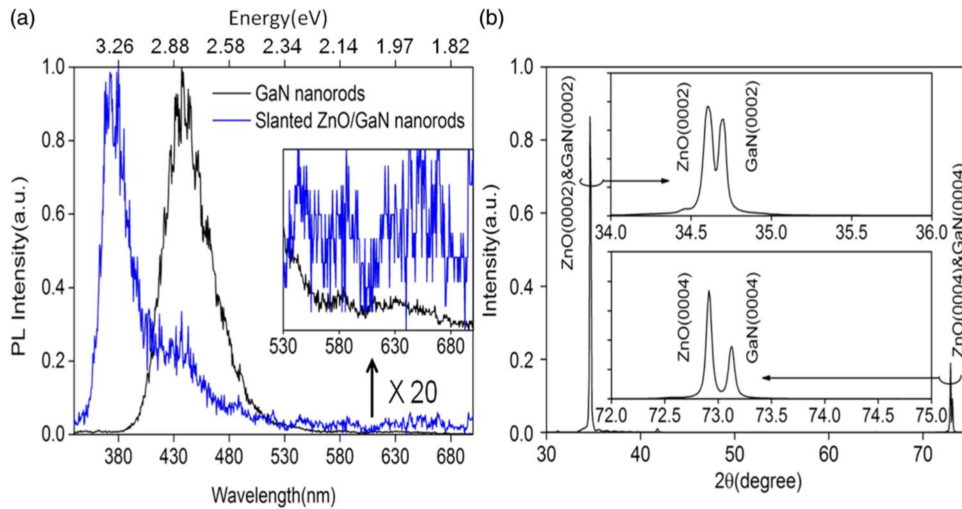

FIG. 3. (a) PL spectra of p-GaN nanorod arrays with (blue line) and without (black line) slanted ZnO film grown on it. (Inset) 20 times magnification of PL spectra in wavelength region from 530 to 700 nm. (b) XRD (θ–2θ) pattern of the slanted n-ZnO/p-GaN nanorod arrays.

LED with a chip size of 300 μm × 400 μm, and the inset shows an enlarged SEM image of the top surface of slanted ITO layer. A continuous and porous morphology was observed on the LED's surface, and the measured roughness (root-mean-square, RMS) by atomic force microscopy is about RMS = 45 nm, as shown in Fig. 1(c).

The photoluminescence (PL) and X-ray diffraction (XRD) measurements were performed to characterize the crystalline quality of our nanorod LEDs. Figure 3(a) shows the room temperature normalized PL spectra of p-GaN nanorod arrays with (blue line) and without (black line) slanted ZnO film grown on it. The 325 nm He-Cd continuous wave laser with a spot size of ∼100 μm was used as an excitation source. The PL spectrum of p-GaN nanorod arrays exhibits a blue emission with a peak wavelength around $\lambda = 440$ nm, which is commonly observed and mainly attributed to the transitions from the conduction band or shallow donors to Mg acceptors levels in p-GaN. After the growth of slanted ZnO film on p-GaN nanorod arrays, a sharp and dominant UV emission centered at $\lambda = 380$ nm with a full width at half maximum (FWHM) of 30 nm was clearly observed, corresponding to the near-band-edge (NBE) transition of ZnO. The secondary peak centered at $\lambda = 440$ nm results from p-GaN nanorod arrays directly under the slanted ZnO film. The inset of Fig. 3(a) shows the magnified intensity (20X) of PL spectra in wavelength region from 530 to 700 nm, in which a very weak and broad luminescence attributable to the defect-related transitions of ZnO could be observed.[11] Above observation on PL spectra indicates a relatively low defect and impurity concentrations in the slanted ZnO film, which is beneficial to enhance the probability of photon emission with energy near the ZnO NBE. Figure 3(b) shows XRD (θ–2θ) patterns of slanted n-ZnO/p-GaN nanorod arrays. Accordingly, the diffraction peaks of slanted n-ZnO/p-GaN nanorod arrays exhibit the crystallographic wurtzite structure along *c*-axis orientation. Two close but distinguishable diffraction peaks are clearly observed around 34° (also 73°) corresponding to the orientations in the (0002) plane ((0004) plane) of ZnO and GaN. The corresponding FWHM of the XRD rocking curves are also similar, which are 0.059° and 0.055°, and 0.063° and 0.065°, for the (0002) and (0004) planes of ZnO and GaN, respectively. Most importantly, the intensity of diffraction peaks of ZnO is stronger than that of GaN, suggesting the slanted ZnO film is of good crystalline quality, low interfacial defect, and monocrystalline nature, which agrees well with the measured PL spectra shown in Fig. 3(a).

To characterize the electrical properties of our slanted n-ZnO/p-GaN nanorod arrays, current versus voltage (*I-V*) curve was measured by a Keithley 2400 electrometer at room temperature. According to the *I-V* curve shown in Fig. 4(a), the slanted n-ZnO/p-GaN nanorod arrays exhibit a well rectifying diode-like behavior with a turn-on voltage of 4.7 V, indicating a proper formation of

This article is copyrighted as indicated in the article. Reuse of AIP content is subject to the terms at: http://aplmaterials.aip.org/about/rights_and_permissions Downloaded to IP: 140.113.38.11 On: Thu, 25 Dec 2014 02:59:18

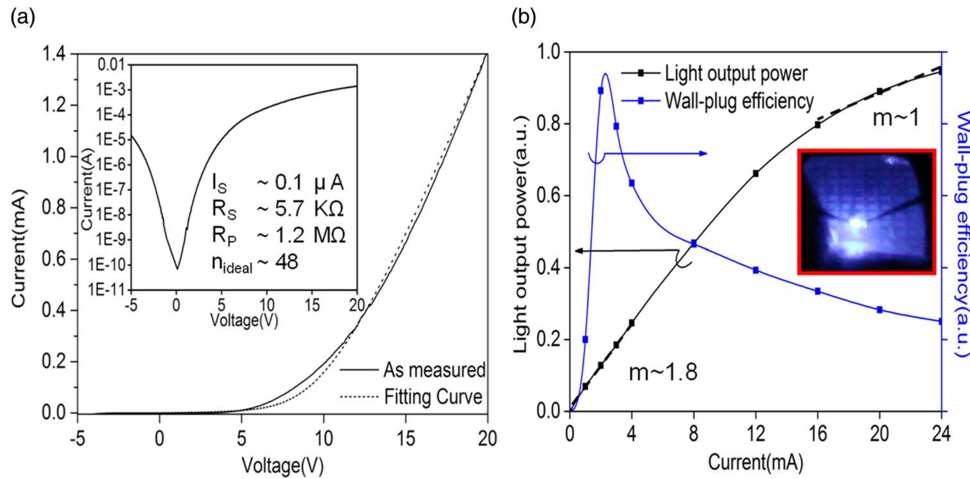

FIG. 4. (a) Current vs. voltage (*I-V*) behavior of the slanted n-ZnO/p-GaN nanorod arrays LED. (Inset) The same *I-V* current plotted in a semi-log scale. The series (R_S) and shunt (R_P) resistances, and the saturated current (I_S) and ideality factor (n_{ideal}) extracted from the *I-V* curve are also summarized in the figure. (b) Light output power and wall-plug efficiency vs. forward injection current of the slanted n-ZnO/p-GaN nanorod arrays LED. (Inset) A photography of actual device operating at an injection current of $I = 12$ mA.

nanosized p-n heterojunction. The measured rectifying *I-V* curve was well described by the modified Shockley equation:[23]

$$I - [(V - IR_S)/R_P] = I_S \exp[q(V - IR_S)/(n_{ideal}kT)], \tag{1}$$

where n_{ideal} and I_S represent the ideality factor and saturation current, respectively. R_S and R_P are the series and shunt resistances, respectively. The series and shunt resistances, and the ideality factor and saturation current extracted by Eq. (1) are estimated to be $R_S = 5.7$ kΩ and $R_P = 1.2$ MΩ, and $n_{ideal} = 48$ and $I_S = 0.1$ μA, respectively. The inset of Fig. 4(a) re-plots the *I-V* curve in a semi-log scale to identify the value of leakage current. Accordingly, the leakage current in the order of 1.5 $\times$ 10^{-5} A at -5 V is measured, which is acceptable for the LED with a chip size of 300 μm $\times$ 400 μm [Fig. 1(b)]. Figure 4(b) shows light output power and wall-plug efficiency versus forward injection current of the LED. A photograph of light emission of slanted n-ZnO/p-GaN nanorod arrays LED at $I = 12$ mA is also inserted in Fig. 4(b). The bluish-white EL is strong enough to be directly observed by naked eyes. Meanwhile, we observe a superlinear dependence on the *L-I* curve at low currents ($I < 4$ mA) with a slope of 1.8 ($L \sim I^m$, $m = 1.8$), and that becomes sublinear ($m = 1.0$) at higher injected currents ($I > 16$ mA). The measured wall-plug efficiency therefore achieves its highest value at low injection current of $I \sim 4$ mA, and then decreases pronouncedly with a further increasing of injection current. The possible reason responsible for the change in the slope and efficiency-droop in the high current could be attributed to device's overheating.

We now examine the EL spectrum of the slanted n-ZnO/p-GaN nanorod arrays LED. Figure 5(a) shows the EL spectra as a function of wavelength for various injection currents, and that was then converted into 3D contour image as depicted in Fig. 5(b). Accordingly, two distinguishable main peaks at $\lambda \sim 390$ nm and $\lambda \sim 485$ nm were identified. The physical origin of the 390 nm emission should be dominated by the ZnO NBE emission (shallow donors to the valence band),[11,18] whereas that of the 485 nm emission is probably related to the radiative interfacial recombination of the electrons from slanted n-ZnO and holes from p-GaN nanorod arrays,[18] or to the energy transition from a shallow donor level to the V_{Zn} level.[24] As the injection current is increased, the EL intensity increases exponentially and the dominant emission peak is slightly blueshifted in the range of 390–415 nm. Since the band bending of energy profile at the interface of n-ZnO and p-GaN is reduced as the injection current increases, the kinetic energy of injected electrons and holes is hence increased, which leads to a higher probability for the radiaive recombinations and generally accompanies with a blueshift behavior. Additionally, the calculated CIE chromaticity ordinates of EL spectra inserted

This article is copyrighted as indicated in the article. Reuse of AIP content is subject to the terms at: http://aplmaterials.aip.org/about/rights_and_permissions Downloaded to IP: 140.113.38.11 On: Thu, 25 Dec 2014 02:59:18

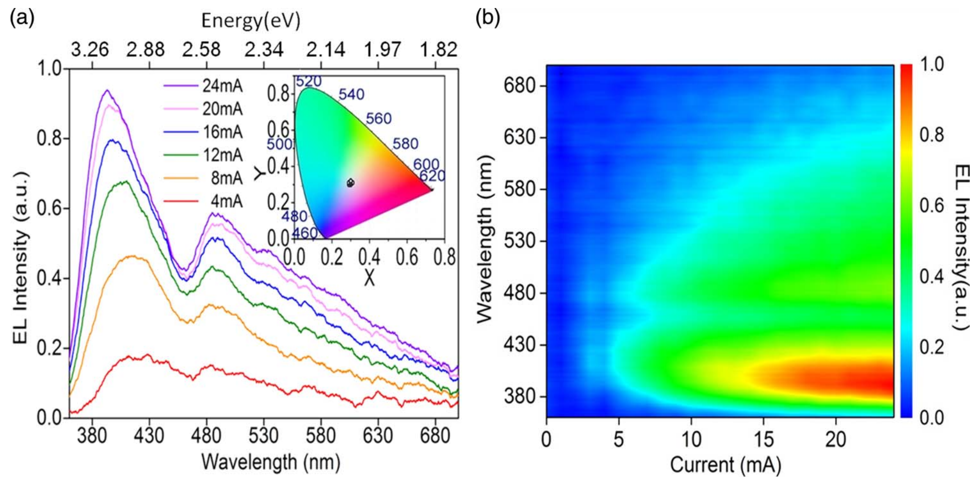

FIG. 5. (a) EL spectra of the slanted n-ZnO/p-GaN nanorod arrays LED for various injection currents. (Inset) Calculated CIE chromaticity ordinates of EL spectra. (b) The same EL spectra converted and re-plotted as 3D contour image.

in Fig. 5(a) are almost identical to (0.30 ± 0.01, 0.30 ± 0.01) regardless of variation of injection currents, exploring the possible application of using such nanorod arrays LED as white-light sources in solid-state lighting.

In summary, we have demonstrated a general scheme for the fabrication of high-efficient ZnO-based nanorod LED arrays by using of oblique-angle deposition. The inclined ZnO vapor-flow was selectively grown on the tip surfaces of pre-fabricated p-GaN nanorod arrays, resulting in the formation of nanosized heterojunctions. The characterization of the fabricated device shows good diode behavior with low turn-on voltage of 4.7 V and strong bluish-white EL emission. Since the device preparation does not involve passivation of using a polymer or sophisticated material growth techniques, we believe the revealed scheme might be directly applied on other kinds of hetero-semiconductor nano-devices.

The authors gratefully acknowledge the financial support from the National Science Council of the Republic of China (ROC) in Taiwan (Contract Nos. NSC–100–2112–M–003–006–MY3, NSC-101-2112-M-019-003-MY3, and NSC 102-2218-E-009-017).

[1] A. Tsukazaki, A. Ohtomo, T. Onuma, M. Ohtani, T. Makino, M. Sumiya, K. Ohtani, S. F. Chichibu, S. Fuke, Y. Segawa, H. Ohno, H. Koinuma, and M. Kawasaki, Nat. Mater. **4**, 42 (2005).
[2] D. M. Bagnall, Y. F. Chen, Z. Zhu, T. Yao, M. Y. Shen, and T. Goto, Appl. Phys. Lett. **73**, 1038 (1998).
[3] Z. L. Wang, J. Phys.: Condens. Mat. **16**, R829 (2004).
[4] M. Joseph, H. Tabata, and T. Kawai, Jpn. J. Appl. Phys. Lett. **38**, L1205 (1999).
[5] C. Y. Huang, Y. J. Lee, T. Y. Lin, S. L. Chang, J. T. Lian, H. M. Lin, N. C. Chen, and Y. J. Yang, Opt. Lett. **39**, 805 (2014).
[6] B. Xiang, P. W. Wang, X. Z. Zhang, S. A. Dayeh, D. P. R. Aplin, C. Soci, D. P. Yu, and D. L. Wang, Nano Lett. **7**, 323 (2007).
[7] A. Khan, K. Balakrishnan, and T. Katona, Nat. Photon. **2**, 77 (2008).
[8] Ya. I. Alivov, J. E. Van Nostrand, D. C. Look, M. V. Chukichev, and B. M. Ataev, Appl. Phys. Lett. **83**, 2943 (2003).
[9] S. J. An and G. C. Yi, Appl. Phys. Lett. **91**, 123109 (2007).
[10] C. Bayram, F. H. Teherani, D. J. Rogers, and M. Razeghi, Appl. Phys. Lett. **93**, 081111 (2008).
[11] H. Huang, G. Fang, Y. Li, S. Li, X. Mo, H. Long, H. Wang, D. L. Carroll, and X. Zhao, Appl. Phys. Lett. **100**, 233502 (2012).
[12] X. Y. Liu, C. X. Shan, C. Jiao, S. P. Wang, H. F. Zhao, and D. Z. Shen, Opt. Lett. **39**, 422 (2014).
[13] E. Lai, W. Kim, and P. Yang, Nano Res. **1**, 123 (2008).
[14] T. Nakayama and M. Murayama, J. Cryst. Growth **214–215**, 299 (2000).
[15] W. I. Park and G. C. Yi, Adv. Mater. **16**, 87 (2004).
[16] H. Kim, Y. Cho, H. Lee, S. Kim, S. R. Ryu, D. Y. Kim, T. W. Kang, and K. S. Chung, Nano Lett. **4**, 1059 (2004).
[17] X. W. Sun, J. Z. Huang, J. X. Wang, and Z. Xu, Nano Lett. **8**, 1219 (2008).
[18] S. Xu, C. Xu, Y. Liu, Y. Hu, R. Yang, Q. Yang, J. H. Ryou, H. J. Kim, Za. Lochner, S. Choi, R. Dupuis, and Z. L. Wang, Adv. Mater. **22**, 4749 (2010).
[19] H. K. Fu, C. L. Cheng, C. H. Wang, T. Y. Lin, and Y. F. Chen, Adv. Funct. Mater. **19**, 3471 (2009).
[20] Y. J. Lee, S. Y. Lin, C. H. Chiu, T. C. Lu, H. C. Kuo, S. C. Wang, S. Chhajed, J. K. Kim, and E. F. Schubert, Appl. Phys. Lett. **94**, 141111 (2009).

This article is copyrighted as indicated in the article. Reuse of AIP content is subject to the terms at: http://aplmaterials.aip.org/about/rights_and_permissions Downloaded to IP: 140.113.38.11 On: Thu, 25 Dec 2014 02:59:18

[21] Y. C. Yao, M. T. Tsai, H. C. Hsu, L. W. She, C. M. Cheng, Y. C. Chen, C. J. Wu, and Y. J. Lee, Opt. Exp. **20**, 3479 (2012).
[22] A. M. C. Ng, Y. Y. Xi, Y. F. Hsu, A. B. Djurišić, W. K. Chan, S. Gwo, H. L. Tam, K. W. Cheah, P. W. K. Fong, H. F. Lui, and C. Surya, Nanotechnology **20**, 445201 (2009).
[23] E. F. Schubert, *Light-Emitting Diodes* (Cambridge University, 2006).
[24] A. Janotti and C. G. Van de Walle, Phys. Rev. B **76**(16), 165202 (2007).

This article is copyrighted as indicated in the article. Reuse of AIP content is subject to the terms at: http://aplmaterials.aip.org/about/rights_and_permissions Downloaded to IP: 140.113.38.11 On: Thu, 25 Dec 2014 02:59:18